Nucleation Barriers for the Liquid-To-Crystal Transition in Ni: Experiment and Simulation

J. Bokeloh,[1] R. E. Rozas,[2,3] J. Horbach,[2,3] and G. Wilde[1]

[1]*Institut für Materialphysik, Westfälische Wilhelms-Universität Münster, Wilhelm Klemm-Str. 10, 48149 Münster, Germany*
[2]*Institut für Materialphysik im Weltraum, Deutsches Zentrum für Luft- und Raumfahrt (DLR), 51170 Köln, Germany*
[3]*Institut für Theoretische Physik der Weichen Materie, Heinrich Heine-Universität Düsseldorf, Universitätsstraße 1, 40225 Düsseldorf, Germany*

(Received 26 May 2011; revised manuscript received 21 July 2011; published 26 September 2011)

Nucleation in undercooled Ni is investigated by a combination of differential scanning calorimetry (DSC) experiments and Monte Carlo (MC) simulation. By systematically varying the sample size in the DSC experiments, nucleation rates J over a range of 8 orders of magnitude are obtained. Evidence is given that these rates correspond to homogeneous nucleation. Free energy barriers ΔG^*, as extracted from the measured J, are in very good agreement with those from the MC simulation. The MC simulation indicates a nonspherical geometry of crystalline clusters, fluctuating between prolate and oblate shape at a given size. Nevertheless, the temperature dependence of ΔG^* is well described by classical nucleation theory.

DOI: 10.1103/PhysRevLett.107.145701 PACS numbers: 64.70.D−

Introduction.—Crystal nucleation from an undercooled melt is one of the fundamental processes during solidification [1]. Despite this, even for simple metals such as Ni or model systems such as hard spheres, nucleation is far from being well understood at a microscopic level [2–9].

In the framework of classical nucleation theory (CNT) for homogeneous nucleation, the excess free energy $\Delta G(n)$ to form a spherical nucleus containing n particles is related to *macroscopic* thermodynamic properties such as the bulk chemical potential difference $\Delta\mu$ between crystal and liquid and the interfacial free energy γ for the formation of an interface between crystal of density ρ and melt,

$$\Delta G(n) = -n|\Delta\mu| + 4\pi[3n/(4\pi\rho)]^{2/3}\gamma. \quad (1)$$

Because of the competition of the negative bulk term and the positive surface term, the function $\Delta G(n)$ exhibits a maximum at the critical barrier $\Delta G^* = \frac{16\pi\gamma^3}{3(\rho|\Delta\mu|)^2}$, corresponding to the critical size $n^* = 32\pi\gamma^3/(3|\Delta\mu|^3\rho^2)$. In principle, CNT is expected to hold for a macroscopic size of the nucleus; only then, the surface term can be considered to be proportional to the macroscopic interfacial free energy γ. However, under experimentally relevant values for the undercooling $\Delta T = T_m - T$ (with T the temperature and T_m the melting temperature), the typical size of the critical nucleus may contain only a few hundred atoms and one expects significant correction terms to the free energy balance, as obtained from CNT.

In nucleation experiments of atomistic systems, a direct determination of ΔG^* is not possible and one usually extracts the nucleation barrier from the nucleation rate,

$$J = \Gamma \exp[-\Delta G^*/(k_B T)] \quad (2)$$

with k_B the Boltzmann factor and Γ a kinetic prefactor. The nucleation rate in turn is derived from measurements of the crystallization temperature. To extract the barrier ΔG^*, the kinetic prefactor must either be taken from theoretical estimates [10] or treated as a fit parameter.

In this Letter, we demonstrate for the case of Ni that the combination of differential scanning calorimetry (DSC) experiments and Monte Carlo (MC) simulation can reveal the dependence of ΔG^* on undercooling.

Whereas usually from DSC experiments the nucleation rate is only determined for one temperature, the data presented below encompass a range of 8 orders of magnitude for the nucleation rate. This range could be only covered by broad variation of sample masses and observation time scales. We give evidence that from our experiments we obtain in fact rates J for homogeneous nucleation. From the measurements of J, nucleation barriers ΔG^* are estimated employing the dependence of ΔG^* on undercooling as found from the simulation.

The Monte Carlo (MC) simulations are done in conjunction with umbrella sampling and parallel tempering [11] using an embedded atom method (EAM) potential proposed by Foiles (F85) [12] to model the interactions between the Ni atoms. The barriers ΔG^* obtained from the simulation are in excellent agreement with those from the experiment. The simulations allow us to consider a broad range of undercoolings, $450\ \mathrm{K} \geq \Delta T \geq 250\ \mathrm{K}$, where ΔG^* increases from about 2 to 11 eV. Although $\Delta G(n)$ cannot be described by Eq. (1), we find that ΔG^* obeys a temperature dependence based on CNT,

$$\Delta G^* = BT^3/\Delta T^2. \quad (3)$$

This expression follows from CNT with the additional approximations $|\Delta\mu| = \Delta H_f \Delta T/T_m$ [10] and $\gamma = \gamma_m T/T_m$ [13]. With the heat of fusion $\Delta H_f = 17.29\ \mathrm{kJ/mol}$, the solid density $\rho = 8357\ \mathrm{kg/m^3}$ at T_m and the interfacial free energy at the melting point $\gamma_m = 0.302\ \mathrm{J/m^2}$ from previous simulations of the F85 model [14], the proportionality factor B amounts to

2.72×10^{-4} eV/K. This value overestimates the one obtained from a fit to the MC data for ΔG^* by about 30% (see below). Despite this rather good agreement between MC calculations and CNT, we show that in contradiction to CNT the geometry of the crystalline clusters is nonspherical.

Experiments.—Most of the experimental data for J were obtained from a statistical evaluation of the crystallization behavior during continuous cooling. A single Ni sample was repeatedly heated up to 1773 K and subsequently cooled down to 1373 K at a heating and cooling rate of 30 K/min in a Setaram Labsys DSC. Only the range of low nucleation rates ($< 10^{-4}$ mg^{-1} s^{-1}) was explored by isothermal experiments [1]. The samples were embedded within a small amount of molten glass to remove potent nucleation sites such as oxides and to prevent contact of the liquid sample with the crystalline crucible [15]. The system size was varied by analyzing sample masses from 63 mg down to 23 μg.

For each sample, up to 500 cycles were performed yielding 500 different values of undercooling ΔT (Fig. 1). Note that for the smallest mass of 23 μg it was not possible to obtain more than 80 cycles. From the cooling cycles, we obtained the survivorship function $F_{\mathrm{sur}}(\Delta T)$, defined as the fraction of experiments in which crystallization did not yet occur at a given value of ΔT. By employing that nucleation follows inhomogeneous Poisson statistics [16], the nucleation rate J can be directly determined from the function $F_{\mathrm{sur}}(\Delta T) = 1 - \exp(\int J(\Delta T)dt)$ [15–19]. While the uncertainty of the values from isothermal measurements is about 30%, the determination of nucleation rates from $F_{\mathrm{sur}}(\Delta T)$ provides high statistical accuracy. However, systematic errors were introduced by the measurement of temperature that was determined with a relative error of 0.15 K and an absolute error of 2 K.

In Fig. 2, the nucleation rate $J(\Delta T)$ from the different samples is displayed. The continuous temperature dependence indicates that only one type of nucleation site is active throughout the measurements. Moreover, the smooth transition of J between different sample masses shows that surface nucleation can be discarded as an active mechanism (see also supplemental information [20]). This result is remarkable in the framework of nucleation studies of high-melting materials [1] since most methodologies that rely on applying noncatalytic coatings do not work at high temperatures [1], specifically since the surfaces of high-melting metals are prone to developing active nucleation sites due to their high reactivity. In our experiment, the encasement into a glass serves to isolate the sample from crystalline container walls and enhances the purity of the material through oxide dissolution [15].

In most experimental nucleation studies, impurities as prevalent nucleation sites cannot be completely ruled out. For the present measurements, the purity of Ni was varied from 99.999% to 99.6% without any visible influence on the nucleation rate (Fig. 2). While this is a strong argument against nucleation on impurities, it is not possible to completely dismiss heterogeneous nucleation, since the purity variation does not specifically target any potential nucleation sites. Furthermore, for Ni of similar purity, a higher undercooling value has been reported in the literature [21]. Thus, we cannot completely dismiss that in the present study the obtained undercooling values might be affected by a constant impurity nucleant of low potency.

Also included in Fig. 2 is a fit according to Eqs. (2) and (3). The use of this fit implies that the temperature dependence of $\ln(\Gamma)$ is negligible in the temperature interval $1450\ \mathrm{K} > T > 1410\ \mathrm{K}$. This can be rationalized by recent measurements of the self-diffusion constant of Ni by quasielastic neutron scattering [22]. The results of the fit are $\Gamma = 3.98 \times 10^{23}$ mg^{-1} s^{-1} and $B = 2.14 \times 10^{-4}$ eV/K.

Simulation.—Umbrella sampling was employed to sample nucleation processes [5,11,23] at undercoolings

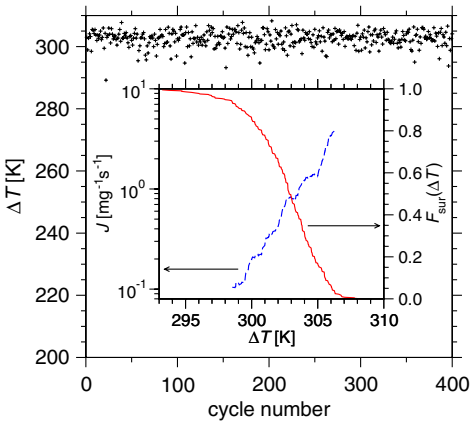

FIG. 1 (color online). Undercooling ΔT, as measured from 400 cycles of a 0.23 mg sample. The inset shows the survivorship function $F_{\mathrm{sur}}(\Delta T)$ (right y axis) and nucleation rate J (left y axis).

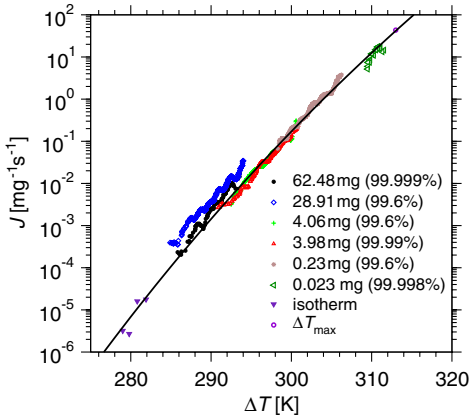

FIG. 2 (color online). Temperature dependence of nucleation rates from the experiments for different system sizes, as indicated. The solid line corresponds to a fit according to Eqs. (2) and (3).

450 K $\geq \Delta T \geq$ 250 K. To this end, the Hamiltonian is modified by the introduction of a harmonic bias potential, $w(n) = 0.5k(n - n_0)^2$, depending on the size n of the biggest crystalline cluster in the system. This bias potential leads to the sampling of the distribution of cluster sizes around the given value n_0. The width of this distribution is controlled by the spring constant k.

To identify crystalline particles, we use a combination of local order parameters. One is the number of particle connections n_c [23]. Two particles i and j are defined as neighbors if the distance between them is less than 3.36 Å (corresponding to first minimum in the radial pair correlation function of the liquid). A pair of neighboring particles is connected if the product $\mathbf{q}_6(i) \cdot \mathbf{q}_6(j) = \sum_{m=-6}^{6} \tilde{q}_{6m}(i)\tilde{q}^*_{6m}(j)$ (with $\tilde{q}_{6m}(i) = \bar{Q}_{6m}(i)/[\sum_{m=-6}^{6} |\bar{Q}_{6m}(i)|^2]^{1/2}$ and $\bar{Q}_{6m}(i)$ the bond order parameter introduced by Steinhardt *et al.* [24]) is larger than 0.5. The second order parameter is the average over neighbors of the product defined above, $q_6q_6(i) = (1/Z_i)\sum_{j=1}^{Z_i} \mathbf{q}_6(i) \cdot \mathbf{q}_6(j)$. A particle i is identified as crystalline if the number of connections, $n_c(i)$, is larger than 7 and the value of $q_6q_6(i)$ larger than 0.6. These threshold values have been identified as the boundary between bulk liquid and crystal in the $q_6q_6 - n_c$ plane.

The Monte Carlo (MC) simulations at constant particle number N, pressure p (at $p = 0$) and temperature T are done in independent windows, specified by different values of n_0. The bias is applied after a trajectory consisting of $5N$ trial displacements and two trial isotropic volume moves. These moves are accepted or rejected in terms of Metropolis criteria [11]. If the latter trajectory of $5N$ trial displacements is rejected the system returns to the configuration from which the trajectory has started. Simulations of different windows were performed in parallel allowing the exchange of bias minima between adjacent windows i and j. This is done every fifth trajectory with probability $\exp(-\beta(w_n - w_o))$ where $w_o = (k_i/2)(n_i - n_{i,0})^2 + (k_j/2)(n_j - n_{j,0})^2$ and $w_n = (k_i/2)(n_i - n_{j,0})^2 + (k_j/2) \times (n_j - n_{i,0})^2$ are the total bias energy of the pair before and after the exchange, respectively. The parameter k_i was set to $k = 0.01$ eV for all windows and the minima $n_{i,0}$ were chosen in steps of 10 to ensure a significant overlap of the cluster size distributions between neighboring windows.

For each window i, the cluster size distribution $P_i(n)$ was used to estimate the excess free energy for the formation of a cluster of size n, $\Delta G_i(n) = -k_B T \ln P_i(n) - w_i(n)$. The results are put in a common frame by adding an offset to $\Delta G_i(n)$ in each window and parameterizing the data by a single polynomial $\Delta G(n) = \sum_{k=1}^{m} a_k n^k$ with $m = 10$. Note that the error bars for the estimate of $\Delta G(n)$ are less than 2%–3% for all values of n.

Figure 3 shows $\Delta G(n)$ at various undercoolings $\Delta T = T_m - T$ and different system sizes N, as indicated. Note that the melting temperature of our EAM model (F85-Ni)

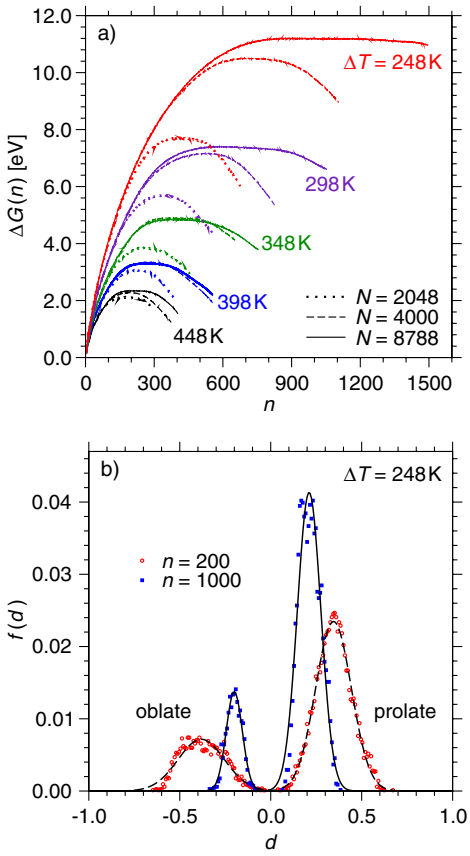

FIG. 3 (color online). (a) Excess free energy, $\Delta G(n)$, for the formation of a cluster of size n for different undercoolings, as obtained from the MC simulation. Three different system sizes with $N = 2048$, $N = 4000$ and $N = 8788$ particles are considered. (b) Distribution $f(d)$ of the deformation parameter d for the cluster sizes $n = 200$ and $n = 1000$ at $\Delta T = 248$ K. The lines are fits with Gaussian functions to each peak.

[12] is at $T_m = 1748$ K [14,25]. The comparison between the three system sizes $N = 2048$, 4000, and 8788 indicates that the system should be at least a factor of 8 larger than the cluster size n in order to avoid finite size effects. The data for $\Delta G(n)$ cannot be described by the CNT prediction, Eq. (1). One reason for this failure of CNT originates from the nonsperical geometry of the crystalline clusters that changes with their size n.

Following Linke *et al.* [26] and Blaak *et al.* [27], we have quantified deviations from a spherical cluster shape in terms of the eigenvalues of the inertia tensor (divided by the mass), $I_{\alpha\beta} = -\sum_{i=1}^{n}(\hat{r}_\alpha^{(i)}\hat{r}_\beta^{(j)} - \delta_{\alpha\beta}\sum_\gamma \hat{r}_\gamma^{(i)}\hat{r}_\gamma^{(i)})$, with $\hat{r}_\alpha^{(i)}$ the αth component ($\alpha = x, y, z$) of the distance vector between particle i and the center of mass of the cluster. A deformation parameter is defined by $d = 1 - 2e_3/(e_1 + e_2)$, with e_1, e_2 and e_3 the eigenvalues of the inertia tensor. e_1 and e_2 are chosen such that $|e_1 - e_2| \leq |e_i - e_j|$ ($i \neq j$). The parameter d vanishes for a sphere, is equal to 1 for the maximum prolate and -1 for the maximum oblate shape [26].

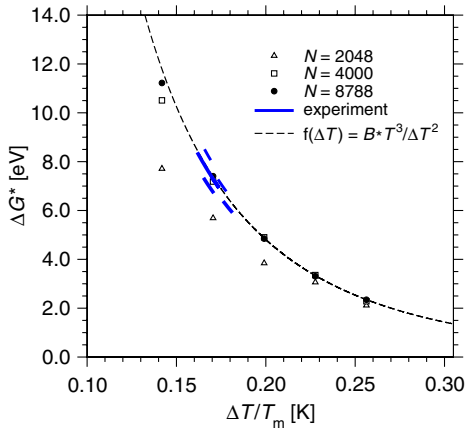

FIG. 4 (color online). ΔG^* as a function of $\Delta T/T_m$. Results from the MC simulation for three different system sizes (symbols) are shown. The experimental data (bold lines) are extracted from the different samples, as indicated in Fig. 2. The dashed line is a fit to simulation data for $N = 8788$ with Eq. (3).

Figure 3(b) shows the probability distribution of the deformation parameter, $f(d)$, for two different cluster sizes $n = 200$ and $n = 1000$ at $\Delta T = 248$ K. These distributions are bimodal, displaying peaks for $d > 0$ and, with a lower amplitude, for $d < 0$. Both peaks move to smaller values of $|d|$ with increasing cluster size. Thus, the clusters fluctuate between prolate and oblate shape (with a higher probability for the prolate geometry) and become more spherical with increasing cluster size. We note that for a given cluster size n the distribution $f(d)$ exhibits only a very weak dependence on undercooling.

The maxima of the function $\Delta G(n)$ correspond to the nucleation barrier ΔG^*, plotted in Fig. 4 as a function of undercooling. The dashed line is a fit with Eq. (3). For the considered range of undercoolings $0.14 \leq \Delta T/T_m \leq 0.26$, the data for the largest system size $N = 8788$ are described very well by this fit function. The fit yields $B = 2.21 \times 10^{-4}$ eV/K. We have also used Eq. (3) to extract ΔG^* from the experimental nucleation rates (Fig. 2). For each sample at a given mass of the system, a separate fit was performed. As a result, the different bold lines in Fig. 4 are obtained; each of them is shown in the range of $\Delta T/T_m$ where the corresponding nucleation rates J for a given system mass were measured.

The fit to the simulation data with Eq. (3) gives $B = 2.21 \times 10^{-4}$ eV/K. The value of B varies from 2.0×10^{-4} eV/K to 2.3×10^{-4} eV/K for the fits to the experimental data. Using ρ, T_m and ΔH_f from the simulation in the CNT expression for B (see above), the latter values for B give an interfacial tension γ_m of the order of 0.275 J/m^2, thus underestimating the direct measurement of γ_m from simulation by about 10% [14].

Conclusions.—Experiments and simulations on the nucleation in undercooled Ni were performed within an overlapping range of undercoolings. For this, a consistent deep undercooling had to be achieved on the experimental side, whereas on the simulation side, the simulation box had to be large enough to prevent finite size effects. The experimental nucleation rates were determined solely from the statistics of crystallization and thus do not rely on any kind of model. The underlying nucleation mechanism is clearly not nucleation on the surface and the independence of the nucleation rate on the sample purity as well as the good agreement to the simulation suggest that indeed homogeneous nucleation was observed.

While the simulations show a deviation of the energy of formation $\Delta G(n)$ from CNT, the actual height of the energy barrier is in good agreement with CNT. This is surprising regarding the nonspherical, fluctuating shape of the clusters. Probably a cancellation of errors leads to the good quantitative description of ΔG^* by CNT.

The authors acknowledge financial support by the German DFG SPP 1296, grant HO 2231/6-2, and WI 1899/5-2. A generous grant of computer time at the NIC Jülich is gratefully acknowledged.

[1] K. F. Kelton and A. L. Greer, *Nucleation in Condensed Matter* (Elsevier, Amsterdam, 2010).
[2] K. Binder, Rep. Prog. Phys. **50**, 783 (1987).
[3] K. Schätzel and B. J. Ackerson, Phys. Rev. E **48**, 3766 (1993).
[4] J. L. Harland and W. van Megen, Phys. Rev. E **55**, 3054 (1997).
[5] S. Auer and D. Frenkel, Nature (London) **409**, 1020 (2001); Nature (London) **413**, 711 (2001); Annu. Rev. Phys. Chem. **55**, 333 (2004).
[6] H. J. Schöpe, G. Bryant, and W. van Megen, Phys. Rev. Lett. **96**, 175701 (2006).
[7] T. Kawasaki and H. Tanaka, Proc. Natl. Acad. Sci. U.S.A. **107**, 14 036 (2010).
[8] W. Lechner, C. Dellago, and P. G. Bolhuis, Phys. Rev. Lett. **106**, 085701 (2011); T. Schilling *et al.*, Phys. Rev. Lett. **105**, 025701 (2010).
[9] L. Filion, R. Ni, D. Frenkel, and M. Dijkstra, J. Chem. Phys. **134**, 134901 (2011).
[10] D. Turnbull, J. Appl. Phys. **21**, 1022 (1950).
[11] D. Frenkel and B. Smit, *Understanding Molecular Simulation* (Academic Press, San Diego, 2001).
[12] S. M. Foiles, Phys. Rev. B **32**, 3409 (1985).
[13] F. Spaepen, Solid State Phys. **47**, 1 (1994).
[14] R. E. Rozas and J. Horbach, EPL **93**, 26 006 (2011).
[15] G. Wilde, J. L. Sebright, and J. H. Perepezko, Acta Mater. **54**, 4759 (2006).
[16] F. G. Yost, J. Cryst. Growth **23**, 137 (1974).
[17] E. A. Gehan, J. Chronic Diseases **21**, 629 (1969).
[18] M. J. Uttormark, J. W. Zanter, and J. H. Perepezko, J. Cryst. Growth **177**, 258 (1997).
[19] G. Wilde *et al.*, J. Phys. Condens. Matter **21**, 464113 (2009).
[20] See Supplemental Material at http://link.aps.org/supplemental/10.1103/PhysRevLett.107.145701 for a comparison of the nucleation rate normalized to the sample surface area.

[21] D. M. Herlach, Annu. Rev. Mater. Sci. **21**, 23 (1991).
[22] A. Meyer *et al.*, Phys. Rev. B **77**, 092201 (2008).
[23] P. R. Ten Wolde, M. J. Ruiz-Montero, and D. Frenkel, Phys. Rev. Lett. **75**, 2714 (1995).
[24] P. J. Steinhardt, D. R. Nelson, and M. Ronchetti, Phys. Rev. B **28**, 784 (1983).
[25] T. Zykova-Timan, R. E. Rozas, J. Horbach, and K. Binder, J. Phys. Condens. Matter **21**, 464102 (2009).
[26] G. T. Linke, R. Lipowsky, and T. Gruhn, Phys. Rev. E **71**, 051602 (2005).
[27] R. Blaak, S. Auer, D. Frenkel, and H. Löwen, Phys. Rev. Lett. **93**, 068303 (2004).